Design, synthesis and photovoltaic properties of two π-bridged cyclopentadithiophene-based polymers

ARTICLE · AUGUST 2014

DOI: 10.1039/C4PY00881B

Polymer Chemistry

PAPER

Cite this: *Polym. Chem.*, 2014, **5**, 6551

Design, synthesis and photovoltaic properties of two π-bridged cyclopentadithiophene-based polymers†

Chuantao Gu,[a,b] Manjun Xiao,[c] Xichang Bao,[a] Liangliang Han,[a] Dangqiang Zhu,[a,b] Ning Wang,[a] Shuguang Wen,[a] Weiguo Zhu*[c] and Renqiang Yang*[a]

Received 24th June 2014,
Accepted 28th July 2014

DOI: 10.1039/c4py00881b

www.rsc.org/polymers

Two fluorinated D–A type conjugated polymers, PCPDT-DTFBT (**P1**) and PCPDT-DTDFBT (**P2**) with an extended π-bridge, were synthesized through the palladium-catalyzed Stille coupling reaction. Both **P1** and **P2** exhibit a narrow band gap (1.63 eV for **P1** and 1.60 eV for **P2**) and low lying energy level with the highest-occupied molecular orbital (HOMO) of −5.16 and −5.19 eV, respectively. Because of the insertion of the 4-hexylthiophene π-bridge between the donor and acceptor units, **P1** and **P2** exhibit excellent solubility in common organic solvents. Particularly for **P2**, the improved solubility was conducive to the film forming ability with a root-mean-square roughness (RMS) value of 3.60 nm and a nanoscale bi-continuous interpenetrating network in the active layer. As a result, a short-circuit current (J_{SC}) of 13.58 mA cm^{-2}, an open circuit voltage (V_{OC}) of 0.70 V, and a fill factor (FF) of 61.6% were obtained, giving a high energy conversion efficiency (PCE) of 5.85% after device optimization.

Introduction

In the past few decades, polymer solar cells (PSCs) have attracted considerable attention for applications in renewable energy due to their low cost, light weight, easy fabrication, and capability of fabricating flexible large-area devices.[1–8] The key factors which determine the power conversion efficiency (PCE) of the PSCs are the open-circuit voltage (V_{OC}), short-circuit current (J_{SC}), and fill factor (FF).[1,9,10] Although the PCE of PSCs has already exceeded 10%,[11] further improvements are needed for mass production and practical applications. One of the most common and successful strategies to improve the PCE is developing new low band gap donor materials.[12,13] The efficient materials should have a low-lying highest occupied molecular orbital (HOMO) energy level to offer high V_{OC}, and good solubility in organic solvents for solution processing.[14,15]

One representative low band gap polymer is poly[4,4-bis(2-ethylhexyl)-4*H*-cyclopenta[2,1-*b*:3,4-*b*′]dithiophene-2,6-diyl-alt-2,1,3-benzothiadiazole-4,7-diyl] (PCPDTBT). The PSCs based on PCPDTBT:[6,6]-phenyl-C_{71}-butyric acid methyl ester ($PC_{71}BM$) showed a moderate PCE of 5.5%, which is mainly limited by the low FF (55%) and low V_{OC} (0.62 V).[7] Recent studies have demonstrated that introducing a strong electron-withdrawing fluorine atom onto the electron-deficient unit of polymers could effectively lower the HOMO energy levels, resulting in increased V_{OC}.[16,17] Moreover, an F atom can form F–H and F–F bonding through intramolecular or intermolecular interactions, which may affect π–π stacking of the polymer to fine-tune its morphology with fullerene, leading to increased J_{SC} and FF.[18–21] Based on this strategy, F-containing PCPDTBT, poly[2,6-(4,4-bis(2-ethylhexyl)-4*H*-cyclopenta[2,1-*b*:3,4-*b*′]dithiophene)-alt-4,7-(5-fluoro-2,1,3-benzothiadiazole)] (PCPDTFBT) and poly[2,6-(4,4-bis(2-ethylhexyl)-4*H*-cyclopenta-[2,1-*b*:3,4-*b*′]dithiophene)-alt-4,7-(difluoro-2,1,3-benzothiadiazole)] (PCPDTDFBT) have been developed by several groups.[22–26] Their encouraging results showed that PCPDTFBT can be a promising low band gap polymer for diverse applications in PSCs. The optimized PCPDTFBT/$PC_{71}BM$ showed a V_{OC} of 0.70–0.77 V, a FF of 48–60% and a PCE between 4.28 and 6.16% with conventional device architecture.[22–26] Although the V_{OC} of fluorinated PCPDTBT has been enhanced, the solubility has been reduced[22,24,25] due to the enhanced F–H and F–F interactions and strong stacking of polymers; the reduced solubility may limit the potential applications of fluorinated PCPDTBT, especially for the PCPDTDFBT, the PCE decreased to 3.37%.[25]

[a]*CAS Key Laboratory of Bio-based Materials, Qingdao Institute of Bioenergy and Bioprocess Technology, Chinese Academy of Sciences, Qingdao 266101, China. E-mail: yangrq@qibebt.ac.cn; Fax: +86-532-80662778; Tel: +86-532-80662700*
[b]*University of Chinese Academy of Sciences, Beijing 100049, China*
[c]*College of Chemistry, Key Lab of Environment-Friendly Chemistry and Application of the Ministry of Education, Xiangtan University, Xiangtan 411105, China. E-mail: zhuwg18@126.com; Fax: +86-731-58292251; Tel: +86-731-58298280*
†Electronic supplementary information (ESI) available: Synthesis details, XRD spectra, detailed device parameters of PSCs and hole mobility. See DOI: 10.1039/c4py00881b

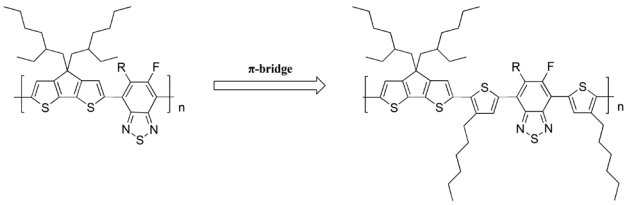

Scheme 1 Structures of **P1** and **P2**.

According to the reported work, thiophene or other heteroaromatic rings can be introduced onto polymers as π-bridges, which can greatly influence the properties of polymers.[27–29] In order to improve the solubility and photovoltaic performance of fluorinated PCPDTBT, the *n*-hexylthiophene unit is introduced onto the fluorinated PCPDTBT as π-bridges in this work. The 4-substituted thiophene shows higher mobility and less steric hindrance compared to 3-substituted thiophene,[30–32] thus in this work 4-substituted thiophene was preferred. The structures of the resulting polymers, PCPDT-DTFBT (here referred to as **P1**) and PCPDT-DTDFBT (here referred to as **P2**), are shown in Scheme 1. The thermal stabilities, photophysical, electrochemical and photovoltaic properties of the polymers were carefully investigated. The **P2**/$PC_{71}BM$ based PSC obtained a promising PCE of 5.85% with higher J_{SC} (13.58 mA cm^{-2}) and FF (61.6%) compared to its PCPDTDFBT/$PC_{71}BM$ analogue (9.59 mA cm^{-2}, 42%).[25]

Experimental

Materials

All reagents and starting materials were purchased from commercial sources and used without further purification unless otherwise noted. All air and water sensitive reactions were performed under a nitrogen atmosphere. Tetrahydrofuran (THF) and toluene were distilled from sodium, with benzophenone as an indicator.

Characterization

^1H NMR spectra were recorded on a Bruker Advance III 600 (600 MHz). Ultraviolet-visible (UV-vis) absorption spectra were recorded at room temperature using a Hitachi U-4100 spectrophotometer. FT-IR spectra were recorded on a Nicolet 6700 spectrophotometer using KBr pellets. Cyclic voltammetry (CV) measurements were performed on a CHI 660D electrochemical workstation equipped with a three-electrode cell consisting of a platinum disk working electrode (2.0 mm in diameter), a saturated calomel reference electrode (SCE) and a platinum wire counter electrode. The measurements were carried out in anhydrous acetonitrile containing 0.1 M tetrabutylammonium phosphorus hexafluoride (Bu_4NPF_6) as the supporting electrolyte under a nitrogen atmosphere at a scan rate of 50 mV s^{-1}. Thin films were deposited from chloroform solution onto the platinum working electrodes and dried under nitrogen prior to measurement. The redox potential of the ferrocene/ferrocenium (Fc/Fc^+) internal reference is 0.39 V *vs.* SCE. HOMO energy levels and the lowest unoccupied molecular orbital (LUMO) were determined by calculating the empirical formula of $E_{HOMO} = -(E_{ox} + 4.80 - E_{1/2,(Fc/Fc^+)})$, $E_{LUMO} = -(E_{red} + 4.80 - E_{1/2,(Fc/Fc^+)})$, where E_{ox} and E_{red} were the onset oxidation and reduction potentials, respectively. Thermogravimetric analysis (TGA) measurements were performed by a STA-409 at a heating rate of 10 °C min^{-1}, under the protection of nitrogen atmosphere. X-ray diffraction (XRD) spectra were recorded on a Bruker D8 Advance spectrometer. Gel permeation chromatography (GPC) analyses were made using THF as the eluant. Surface roughness and morphology of thin films were characterized by atomic force microscopy (AFM) on an Agilent 5400.

Device fabrication

Photovoltaic devices were fabricated on 15 mm × 15 mm patterned indium tin oxide (ITO) coated glass substrates with a layered structure of ITO/PEDOT : PSS (40 nm)/polymer : $PC_{71}BM$ blend (~110 nm)/Ca (10 nm)/Al (100 nm). The ITO coated glass substrates were cleaned in an ultrasonic bath in acetone, methanol and isopropyl alcohol sequentially. The substrates were treated by oxygen plasma for 6 min, then spin-coated with PEDOT : PSS at 4000 rpm, and annealed in an oven for 20 min at 160 °C. The polymer and $PC_{71}BM$ were dissolved in deoxygenated anhydrous chlorobenzene (CB) in the weight ratios 3 : 2, 5 : 4, 1 : 1 and 1 : 2 and the total concentration of the polymer/$PC_{71}BM$ blending solution was 25 mg mL^{-1}. The solutions were stirred overnight in a nitrogen filled glovebox. An active layer consisting of the blend of the polymer and $PC_{71}BM$ was then spin coated on PEDOT : PSS. Subsequently Ca (10 nm) and Al (100 nm) were thermally evaporated at a vacuum of ~2×10^{-4} Pa on top of the active layer as a cathode. The cathode area defines the active area of the devices, which is 0.1 cm^2. The photovoltaic performance was characterized under illumination with an AM 1.5 G (100 mW cm^{-2}), and current density *vs.* voltage (*J*–*V*) curves were recorded by Keithley 2420. External quantum efficiencies (EQE) of solar cells were analyzed by a certified Newport incident photon conversion efficiency (IPCE) measurement system.

General synthetic procedure of polymers

4,4-Bis(2-ethylhexyl)-2,6-bis(trimethylstannanyl)-4*H*-cyclopenta-[2,1-*b*:3,4-*b*′]dithiophene (CPDT)[33–35] and 4,7-bis(5-bromo-4-hexylthienyl)-5,6-difluoro-2,1,3-benzothiadiazole (DTDFBT)[36] were synthesized according to previously reported methods. The synthesis of 4,7-bis(5-bromo-4-hexylthienyl)-5-fluoro-2,1,3-benzothiadiazole (DTFBT) was depicted in ESI.† Both polymers were prepared by the same procedure through the coupling reaction between CPDT and DTFBT or DTDFBT. In a 25 mL round-bottom flask, CPDT, DTFBT (or DTDFBT), tris(dibenzylideneacetone)dipalladium (6 mg) and tris(*o*-tolyl)phosphine (14 mg) were subjected to three cycles of evacuation/nitrogen purging and then 6 mL of anhydrous toluene was added.

The oil bath was heated to 110 °C carefully, and the reactant was stirred for 36 h at this temperature under a nitrogen atmosphere. The reaction mixture was cooled down to room temperature and precipitated in 150 mL of methanol. The precipitate was filtered and then purified by Soxhlet extraction with methanol, hexane, and $CHCl_3$ in succession. $CHCl_3$ fractions were collected, concentrated, reprecipitated in methanol, and dried under vacuum overnight to offer the target polymers.

P1: CPDT (145.9 mg, 0.200 mmol) and DTFBT (129.0 mg, 0.200 mmol) were used in this polymerization following the general polymerization procedure, and the polymer was obtained as a blue solid (132.2 mg, yield 74.0%). ^{1}H NMR (600 MHz, $CDCl_3$): δ (ppm) 8.12 (br, 1H), 8.00 (br, 1H), 7.72 (br, 1H), 7.15 (br, 2H), 2.90 (br, 4H), 1.97 (br, 4H), 1.77 (br, 2H), 1.46 (br, 12H), 1.06 (br, 20H), 0.79 (br, 18H).

P2: CPDT (141.2 mg, 0.194 mmol) and DTDFBT (128.5 mg, 0.194 mmol) were used in this polymerization following the general polymerization procedure, and the polymer was obtained as a purple solid (143 mg, yield 79.9%). ^{1}H NMR (600 MHz, $CDCl_3$): δ (ppm) 8.13 (br, 2H), 7.15 (br, 2H), 2.87 (br, 4H), 1.96 (br, 4H), 1.76 (br, 2H), 1.44 (br, 12H), 1.04 (br, 20H), 0.77 (br, 18H).

Results and discussion

Synthesis and characterization

P1 and **P2** were prepared by Stille coupling polymerization in good yields, using a $Pd_2(dba)_3$/P(*o*-tol)$_3$ catalytic system. The structures of polymers were determined by ^{1}H NMR spectroscopy, which is consistent with the proposed structures. Both polymers show excellent solubility in common organic solvents, such as chloroform, CB, and *o*-dichlorobenzene (*o*-DCB). The polymers can even be partially soluble in dichloromethane. The good solubility should be attributed to the 4-*n*-hexylthiophene π-bridge. The molecular weight and polydispersity index (PDI) were determined by GPC with calibration against polystyrene standards and THF as an eluant. The number average molecular weights (M_n) of **P1** and **P2** were found to be 14.5 and 10.3 kg mol^{-1}, with PDIs of 1.3 and 1.7, respectively. The crystallinity of the polymer films was investigated using XRD spectra (Fig. S1†). There were no peaks observed for the polymers, indicating their amorphous nature.[14] The thermal stability of the polymers was explored by TGA, as shown in Fig. 1. **P1** and **P2** have good thermal stabilities with onset decomposition temperatures corresponding to 5% weight loss at 384 °C and 400 °C, respectively. Obviously, the thermal stabilities of the polymers are adequate for their applications in PSC devices.

Optical properties

The UV-vis absorption spectra of **P1** and **P2** were investigated in dilute chloroform solutions and in thin films as shown in Fig. 2, and the detailed data are summarized in Table 1. Both polymers in solution show characteristic peaks at the low

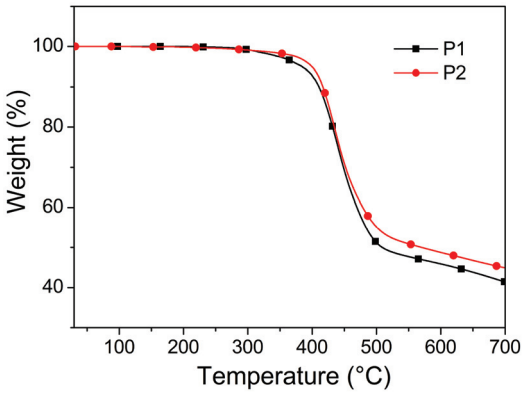

Fig. 1 TGA thermograms of the polymers with a heating rate of 10 °C min^{-1} under a nitrogen atmosphere.

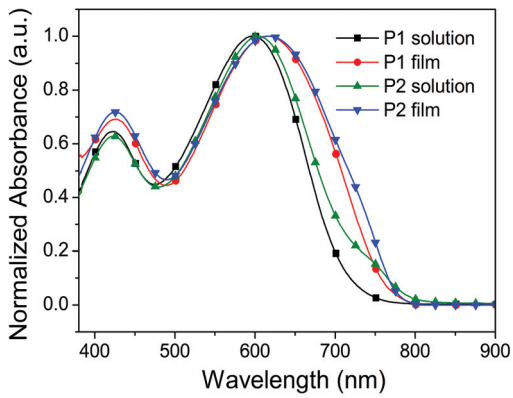

Fig. 2 UV-vis absorption spectra of **P1** and **P2** in chloroform solutions and in thin films.

energy absorption band, which are attributed to the intramolecular charge transfer (ICT) band between donor and acceptor units.[22] In films, the absorption peaks of both polymers are located at about 617 nm. The UV-vis absorption spectra of **P1** and **P2** in films are broader and red-shifted relative to those in solution. This behaviour is ascribed to the enhanced intermolecular interactions between the polymer main chains and the planarization effect of the π-conjugated polymer backbone.[37] The optical band gap (E_g^{opt}) of **P1** and **P2** can be calculated to be 1.63 and 1.60 eV, respectively, from their onset absorption in thin films. It has been proved that attaching a fluorine atom to the electron deficient subunits of low band gap polymers could simultaneously lower the HOMO and LUMO level energies, while having no or only minor effect on E_g^{opt}.[19,24,38] The slight difference of the E_g^{opt} of **P1** and **P2** is in agreement with previously reported results.[18] Compared with PCPDTFBT (1.44 eV) and PCPDTDFBT (1.37 eV),[25] the E_g^{opt} of **P1** and **P2** become bigger which could be ascribed to the more twisted polymer backbone and the weaker electron donating ability of the extended conjugating length of the donor unit in **P1** and **P2** compared to the cyclopenta[2,1-*b*;3,4-*b*′]dithiophene unit in PCPDTFBT and PCPDTDFBT.

Table 1 Optical, electrochemical and thermal properties of **P1** and **P2**

	Solution[a]		Thin film			CV			Thermal
	λ_{max} (nm)	λ_{onset} (nm)	λ_{max} (nm)	λ_{onset} (nm)	$E_g^{opt\ b}$ (eV)	E_{on}^{red}/LUMO (V eV^{-1})	E_{on}^{ox}/HOMO (V eV^{-1})	E_g^{EC} (eV)	T_d (°C)
P1	597	713	617	761	1.63	−0.89/−3.52	0.75/−5.16	1.64	384
P2	605	750	617	775	1.60	−0.96/−3.45	0.78/−5.19	1.74	400

[a] Absorption data were collected in $CHCl_3$ solution. [b] Data were taken by the absorption edge of the thin film, $E_g^{opt} = 1240/\lambda_{onset}$.

Electrochemical properties

The LUMO and HOMO energy levels of the polymers are crucial for the selection of appropriate acceptor materials in active blends in PSCs. CV was employed to evaluate the electrochemical properties and electronic energy levels of both polymers. The energy level of SCE was calibrated against the Fc/Fc^+ system to be 4.41 eV in this work. As shown in Fig. 3a, both polymers show reversible oxidation behaviours. The onset of oxidation and reduction of **P1** was observed at +0.75 and −0.89 V *vs.* SCE, corresponding to HOMO and LUMO levels at −5.16 and −3.52 eV. For **P2**, the onsets were observed at +0.78 and −0.96 V, corresponding to HOMO and LUMO levels at −5.19 and −3.45 eV. Relevant data are summarized in Table 1. The HOMO of **P2** is slightly lower than that of **P1**, which is caused by the two strong electron-withdrawing F atoms. Therefore, a higher V_{OC} in **P2**-based PSCs can be expected, since V_{OC} is proportional to the offset between the HOMO of the polymeric donor and the LUMO of the fullerene acceptor.[38] In order to make a clear comparison, the electronic energy level diagram of **P1**, **P2**, and $PC_{71}BM$ is described in Fig. 3b. The LUMO gaps 0.58 and 0.65 eV between the polymers and $PC_{71}BM$, respectively, are large enough to overcome the intrachain exciton binding energy and thus guarantee efficient exciton dissociation and transfer.[38–40]

Photovoltaic performance

In order to investigate the potential applications of the two polymers in solar cells, the bulk heterojunction PSCs were fabricated with a device structure of ITO/PEDOT : PSS/polymer : $PC_{71}BM$/Ca/Al, and tested under a simulated AM 1.5 G illumination of 100 mW cm^{-2}. The blends of polymer and $PC_{71}BM$ at different weight ratios of 3 : 2, 5 : 4, 1 : 1 and 1 : 2 were used to optimize the device performance. The other conditions, such as spin-coating speed and additive, were also carefully optimized. The *J–V* curves are shown in Fig. 4, and the detailed device parameters are summarized in Tables 2 and S1.† The V_{OC}, which is related to the differences between the HOMO levels of the donor polymers and the LUMO level of the acceptor ($PC_{71}BM$), are found to be 0.75 and 0.79 V for **P1** : $PC_{71}BM$ (5 : 4) and **P2** : $PC_{71}BM$ (5 : 4) devices, respectively. Theoretically achievable V_{OC} of our PSC devices could be calculated according to the equation:

$$V_{OC} = (1/e)(|E^{donor}HOMO| - |E^{PCBM}LUMO|) - 0.3\ V$$

where e is the elementary charge and using −4.1 eV for the $PC_{71}BM$ LUMO energy.[22] The theoretical V_{OC} values of **P1** : $PC_{71}BM$ (5 : 4) and **P2** : $PC_{71}BM$ (5 : 4) devices are 0.76 and 0.79 V, respectively. The experimental V_{OC} values of the polymer devices are in good agreement with the theoretical

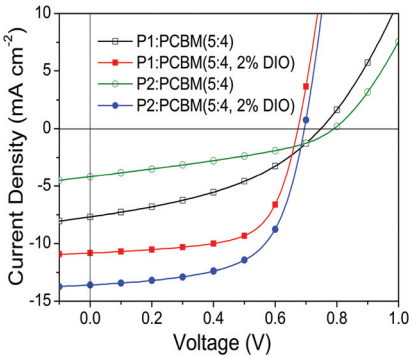

Fig. 4 *J–V* curves of polymer/$PC_{71}BM$-based regular single solar cells under AM 1.5 G illumination, 100 mW cm^{-2}.

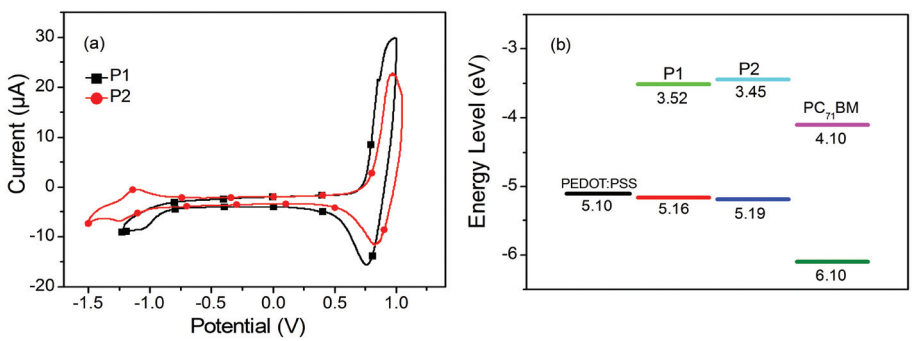

Fig. 3 Cyclic voltammograms (a) and the energy level diagram (b) of **P1** and **P2**.

Table 2 PSC performance with device configuration ITO/PEDOT : PSS/polymer : $PC_{71}BM$/Ca/Al

Active layer	Ratio	DIO (%)	V_{OC} (V)	J_{SC} (mA cm^{-2})	FF (%)	PCE (%)
P1 : $PC_{71}BM$	5 : 4	0	0.75	7.68	40.2	2.32
	5 : 4	2	0.67	10.88	64.6	4.71
P2 : $PC_{71}BM$	5 : 4	0	0.79	4.17	36.2	1.19
	5 : 4	2	0.70	13.58	61.6	5.85

ones. One can observe that the V_{OC} of **P2** is slightly higher than that of **P1**, which could be ascribed to the low lying HOMO of **P2**, and the result agrees well with the energy level obtained from CV. The addition of 1,8-diiodooctane (DIO) to the blend solution is found to greatly increase J_{SC} and FF, and surprisingly enhance PCE doubly. The V_{OC} of both polymers were reduced with the addition of 2% DIO, which is in accordance with previous studies.[1,2,4,24,41] Finally, the highest PCE of 5.85% for **P2** is obtained with a V_{OC} of 0.70 V, a J_{SC} of 13.58 mA cm^{-2}, and an FF of 61.6%, when the device was fabricated at a donor–acceptor weight ratio of 5 : 4 in CB with a total concentration of 25 mg mL^{-1} containing 2% DIO as an additive, spin-cast at 1250 rpm. After the introduction of *n*-hexylthiophene, the J_{SC} and FF of **P2** increased while the V_{OC} decreased when compared with PCPDTDFBT (V_{OC} = 0.84 V, J_{SC} = 9.59 mA cm^{-2}, FF = 42%), as a result the PCE increased from 3.37%[25] to 5.85%. The improvement of photovoltaic performance should be attributed to the introduction of the *n*-hexyl substituted thiophene π-bridge, which also improves the solubility, obviously.

EQE curves of the devices based on both polymers prepared through the optimal fabrication processes are shown in Fig. 5. It can be seen that the devices exhibit broad response over the range 310–780 nm. The EQE value between 390 and 650 nm for the **P2** device exceeded 55% which is higher than that of the **P1** device. The integrated J_{SC} from EQE is 10.57 and 13.33 mA cm^{-2}, respectively, for **P1** and **P2** devices, which are consistent with the measured J_{SC}. Mobility measurements *via* the space charge limited current (SCLC) method[42,43] disclose a hole mobility of 5.1 × 10^{-4} cm^2 V^{-1} s^{-1} for the **P2** : $PC_{71}BM$ device, higher than that of the **P1** : $PC_{71}BM$ device (3.6 × 10^{-4} cm^2 V^{-1} s^{-1}) (Fig. S2†). This could be a potential reason that the **P2** : $PC_{71}BM$ device exhibits larger J_{SC} compared to the **P1** : $PC_{71}BM$ device.

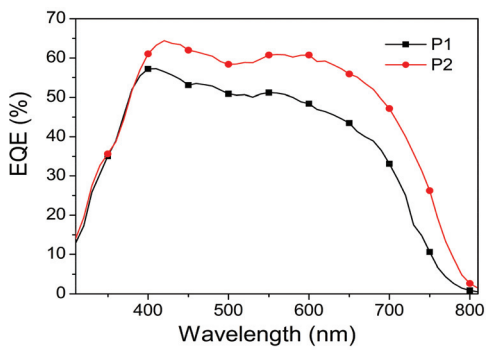

Fig. 5 EQE curves for blends of **P1** and **P2** with $PC_{71}BM$ (5 : 4) processed from CB solution with 2% DIO.

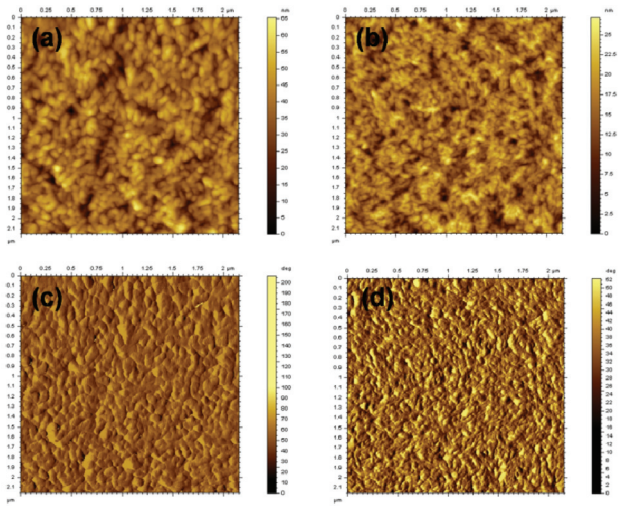

Fig. 6 AFM height (top) and phase (bottom) images of **P1** : $PC_{71}BM$ (a, c) and **P2** : $PC_{71}BM$ (b, d) cast from CB with 2% DIO.

Morphology study

Film surface morphology plays a key role in the efficiency of bulk heterojunction PSCs. AFM images of the active layer surface for the best performance PSCs were collected (Fig. 6). The scan size is 2 μm × 2 μm. The obtained root-mean-square roughness (RMS) values are 7.98 and 3.60 nm for the blend films of **P1** and **P2** with $PC_{71}BM$, respectively. The rougher surface of **P1** may induce poorer contact between the active layer and the cathode, which could lead to a smaller J_{SC}.[44,45] Moreover, from the phase images (Fig. 6c and d) one can clearly observe that **P2**/$PC_{71}BM$ film formed nanoscale phase separation with appropriate domain sizes while **P1**/$PC_{71}BM$ film showed large scale phase separation. And this could be another reason that **P2** exhibits a larger J_{SC} compared to **P1**.

Conclusion

The 4-substituted *n*-hexylthiophene as a π-bridge was introduced to fluorinated PCPDTBTs in order to improve their solubility and nanoscale phase separation in the active layer. The resulting polymers **P1** and **P2** exhibit excellent solubility and good thermal stability with decomposition temperatures higher than 380 °C. Both **P1** and **P2** show narrow E_g^{opt} of 1.63 and 1.60 eV with deep lying HOMO energy levels of −5.16 and −5.19 eV, respectively. The HOMO of **P2** is slightly lower than that of **P1**, resulting in higher V_{OC}. The photovoltaic properties of the polymers were carefully optimized with different polymer/$PC_{71}BM$ weight ratios and additive volume ratio. For the optimized blend of **P2**, a J_{SC} of 13.58 mA cm^{-2}, a V_{OC} of 0.70 V, and an FF of 61.6% are obtained, resulting a high PCE of 5.85%. A device based on **P2** : $PC_{71}BM$ showed higher EQE

and nanoscale interpenetrating morphology in the active layer compared to **P1**-based device. This could partially explain that **P2** exhibits better performance than **P1**. More efforts to optimize the devices based on the polymers are currently undergoing in our group.

Acknowledgements

This work was supported by National Natural Science Foundation of China (21202181, 21204097, 51173199, 51211140346 and 61107090), Ministry of Science and Technology of China (2014CB643501, 2010DFA52310), and Department of Science and Technology of Shandong Province (ZR2012BQ021).

Notes and references

1 M. Zhang, Y. Gu, X. Guo, F. Liu, S. Zhang, L. Huo, T. P. Russell and J. Hou, *Adv. Mater.*, 2013, **25**, 4944–4949.
2 M. Zhang, X. Guo, W. Ma, S. Zhang, L. Huo, H. Ade and J. Hou, *Adv. Mater.*, 2014, **26**, 2089–2095.
3 J. Yuan, Z. Zhai, H. Dong, J. Li, Z. Jiang, Y. Li and W. Ma, *Adv. Funct. Mater.*, 2013, **23**, 885–892.
4 H.-C. Chen, Y.-H. Chen, C.-C. Liu, Y.-C. Chien, S.-W. Chou and P.-T. Chou, *Chem. Mater.*, 2012, **24**, 4766–4772.
5 Y. J. Cheng, S. H. Yang and C. S. Hsu, *Chem. Rev.*, 2009, **109**, 5868–5923.
6 M. C. Scharber and N. S. Sariciftci, *Prog. Polym. Sci.*, 2013, **38**, 1929–1940.
7 J. Peet, J. Y. Kim, N. E. Coates, W. L. Ma, D. Moses, A. J. Heeger and G. C. Bazan, *Nat. Mater.*, 2007, **6**, 497–500.
8 J. Y. Kim, K. Lee, N. E. Coates, D. Moses, T. Q. Nguyen, M. Dante and A. J. Heeger, *Science*, 2007, **317**, 222–225.
9 J. C. Bijleveld, M. Shahid, J. Gilot, M. M. Wienk and R. A. J. Janssen, *Adv. Funct. Mater.*, 2009, **19**, 3262–3270.
10 L. Huo, S. Zhang, X. Guo, F. Xu, Y. Li and J. Hou, *Angew. Chem., Int. Ed.*, 2011, **50**, 9697–9702.
11 J. You, L. Dou, K. Yoshimura, T. Kato, K. Ohya, T. Moriarty, K. Emery, C. C. Chen, J. Gao, G. Li and Y. Yang, *Nat. Commun.*, 2013, **4**, 1446.
12 L. Huo, X. Guo, S. Zhang, Y. Li and J. Hou, *Macromolecules*, 2011, **44**, 4035–4037.
13 Z. He, C. Zhong, X. Huang, W. Y. Wong, H. Wu, L. Chen, S. Su and Y. Cao, *Adv. Mater.*, 2011, **23**, 4636–4643.
14 C.-H. Chen, C.-H. Hsieh, M. Dubosc, Y.-J. Cheng and C.-S. Hsu, *Macromolecules*, 2010, **43**, 697–708.
15 T. Y. Chu, J. Lu, S. Beaupre, Y. Zhang, J. R. Pouliot, S. Wakim, J. Zhou, M. Leclerc, Z. Li, J. Ding and Y. Tao, *J. Am. Chem. Soc.*, 2011, **133**, 4250–4253.
16 Y. Liang, Z. Xu, J. Xia, S. T. Tsai, Y. Wu, G. Li, C. Ray and L. Yu, *Adv. Mater.*, 2010, **22**, E135–E138.
17 H. Zhou, L. Yang, A. C. Stuart, S. C. Price, S. Liu and W. You, *Angew. Chem., Int. Ed.*, 2011, **50**, 2995–2998.
18 A. C. Stuart, J. R. Tumbleston, H. Zhou, W. Li, S. Liu, H. Ade and W. You, *J. Am. Chem. Soc.*, 2013, **135**, 1806–1815.
19 S. C. Price, A. C. Stuart, L. Yang, H. Zhou and W. You, *J. Am. Chem. Soc.*, 2011, **133**, 4625–4631.
20 H. Bronstein, J. M. Frost, A. Hadipour, Y. Kim, C. B. Nielsen, R. S. Ashraf, B. P. Rand, S. Watkins and I. McCulloch, *Chem. Mater.*, 2013, **25**, 277–285.
21 J. Min, Z.-G. Zhang, S. Zhang and Y. Li, *Chem. Mater.*, 2012, **24**, 3247–3254.
22 Y. Zhang, J. Zou, C.-C. Cheuh, H.-L. Yip and A. K. Y. Jen, *Macromolecules*, 2012, **45**, 5427–5435.
23 C.-Y. Chang, L. Zuo, H.-L. Yip, Y. Li, C.-Z. Li, C.-S. Hsu, Y.-J. Cheng, H. Chen and A. K. Y. Jen, *Adv. Funct. Mater.*, 2013, **23**, 5084–5090.
24 S. Albrecht, S. Janietz, W. Schindler, J. Frisch, J. Kurpiers, J. Kniepert, S. Inal, P. Pingel, K. Fostiropoulos, N. Koch and D. Neher, *J. Am. Chem. Soc.*, 2012, **134**, 14932–14944.
25 Y. Li, J. Zou, H.-L. Yip, C.-Z. Li, Y. Zhang, C.-C. Chueh, J. Intemann, Y. Xu, P.-W. Liang, Y. Chen and A. K. Y. Jen, *Macromolecules*, 2013, **46**, 5497–5503.
26 C.-Y. Chang, L. Zuo, H.-L. Yip, C.-Z. Li, Y. Li, C.-S. Hsu, Y.-J. Cheng, H. Chen and A. K. Y. Jen, *Adv. Energy Mater.*, 2014, **4**, 1301645.
27 X. Guo, M. Zhang, L. Huo, F. Xu, Y. Wu and J. Hou, *J. Mater. Chem.*, 2012, **22**, 21024–21031.
28 S. Zhang, L. Ye, Q. Wang, Z. Li, X. Guo, L. Huo, H. Fan and J. Hou, *J. Phys. Chem. C*, 2013, **117**, 9550–9557.
29 X. Wang, Y. Sun, S. Chen, X. Guo, M. Zhang, X. Li, Y. Li and H. Wang, *Macromolecules*, 2012, **45**, 1208–1216.
30 S. k. Lee, S. Cho, M. Tong, J. H. Seo and A. J. Heeger, *J. Polym. Sci., Part A: Polym. Chem.*, 2011, **49**, 1821–1829.
31 H. Zhou, L. Yang, S. Xiao, S. Liu and W. You, *Macromolecules*, 2010, **43**, 811–820.
32 Z. G. Zhang, J. Min, S. Zhang, J. Zhang, M. Zhang and Y. Li, *Chem. Commun.*, 2011, **47**, 9474–9476.
33 Z. Zhu, D. Waller, R. Gaudiana, M. Morana, D. Mühlbacher, M. Scharber and C. Brabec, *Macromolecules*, 2007, **40**, 1981–1986.
34 M. Helgesen and F. C. Krebs, *Macromolecules*, 2010, **43**, 1253–1260.
35 K.-C. Li, J.-H. Huang, Y.-C. Hsu, P.-J. Huang, C.-W. Chu, J.-T. Lin, K.-C. Ho, K.-H. Wei and H.-C. Lin, *Macromolecules*, 2009, **42**, 3681–3693.
36 N. Wang, Z. Chen, W. Wei and Z. Jiang, *J. Am. Chem. Soc.*, 2013, **135**, 17060–17068.
37 X. Sun, W. Chen, Z. Du, X. Bao, G. Song, K. Guo, N. Wang and R. Yang, *Polym. Chem.*, 2013, **4**, 1317–1322.
38 H.-Y. Chen, J. Hou, S. Zhang, Y. Liang, G. Yang, Y. Yang, L. Yu, Y. Wu and G. Li, *Nat. Photonics*, 2009, **3**, 649–653.
39 L. Dou, C.-C. Chen, K. Yoshimura, K. Ohya, W.-H. Chang, J. Gao, Y. Liu, E. Richard and Y. Yang, *Macromolecules*, 2013, **46**, 3384–3390.

40 L. J. A. Koster, V. D. Mihailetchi and P. W. M. Blom, *Appl. Phys. Lett.*, 2006, **88**, 093511.
41 H.-S. Chung, W.-H. Lee, C. E. Song, Y. Shin, J. Kim, S. K. Lee, W. S. Shin, S.-J. Moon and I.-N. Kang, *Macromolecules*, 2014, **47**, 97–105.
42 Y. Chen, Z. Du, W. Chen, Q. Liu, L. Sun, M. Sun and R. Yang, *Org. Electron.*, 2014, **15**, 405–413.
43 S. C. Price, A. C. Stuart and W. You, *Macromolecules*, 2010, **43**, 4609–4612.
44 X. Zhang, L. Sun, W. Zheng, X. Bao, N. Wang, T. Wang and R. Yang, *Tetrahedron*, 2013, **69**, 9544–9550.
45 Q. Liu, X. Bao, S. Wen, Z. Du, L. Han, D. Zhu, Y. Chen, M. Sun and R. Yang, *Polym. Chem.*, 2014, **5**, 2076–2082.